



J. Serb. Chem. Soc. 90 (2) 233–245 (2025)
JSCS–5832

Enhancing fire resistance in wood with high-water retention silica gel: A promising flame-retardant solution

ZHONGBIN FEI, YINGNAN ZHANG, ZHI WANG, YILING DUAN and BIN ZHANG*

*International Center for Chemical Process Safety, Nanjing Tech University, Nanjing,
211816, China*

(Received 14 April, revised 10 June, accepted 23 August 2024)

Abstract: This study aims to evaluate water retention and flame-retardant properties of silica gel prepared using anionic polyacrylamide (HPAM), gluconate-delta-lactone (GDL) and aluminum citrate (AlCit). Silica gel samples were synthesized with sodium silicate (8 wt. %), sodium bicarbonate (4 wt. %) and varying concentrations of HPAM (0.2–0.8 wt. %) and GDL (0.1–0.3 wt. %). The prepared gels were characterized using XPS, XRD, FTIR and TGA. Optimal water retention capacity was achieved with 0.4 wt. % HPAM and 0.2 wt. % GDL. Compared to traditional gels, silica gel has more surface water molecules due to the additional hydrophilic groups and the amorphous nature of silica. At high temperatures, silica forms a layer with the charcoal from treated wood combustion, inhibiting oxygen penetration and minimizing further combustion. After combustion at 500 °C, the mass loss of wood treated with silica gel is 36–53 % less than untreated wood, indicating greater weight retention and demonstrating silica gel's effectiveness in preventing continued burning.

Keywords: polyacrylamide; microscopic process; combustion morphology; mass loss; amorphous silica.

INTRODUCTION

Wood plays a vital role in human life due to its unique properties such as porosity, anisotropy, wet swelling, dry shrinkage, combustion and biodegradability.¹ The wood processing industry in China encompasses several key sectors, including sawn timber processing, wood chip processing, veneer processing, other wood processing, wood-based panel production and wood products manufacturing, with products like construction timber and wooden furniture. In 2022, China's timber output reached 106.93 million m³, comprising 92.44 million m³ of logs and 14.49 million m³ of fuelwood.

* Corresponding author. E-mail: bzhang@njtech.edu.cn
<https://doi.org/10.2298/JSC240414077F>

However, wood's flammability poses risks in building, furniture and decorative items, leading to fire spread and the production of smoke and gases such as carbon monoxide, which can be fatal. Treating wood with a fire retardant is crucial to reduce its combustibility.² One of the oldest flame retardants, borates, is still in use due to its low toxicity and volatility. However, boron compounds' tendency to leach from wood surfaces and interiors under specific conditions poses challenges.³ Surface coatings and fixation of pure boron compounds have shown limited effectiveness in reducing leaching.⁴ Additionally, metal salts can be used to reduce smoke production and flammability by promoting the formation of charcoal and reducing tar products.⁵ However, these salts may also leach from treated wood, affecting their long-term efficacy.⁶

Alkaline silicates like sodium silicate and potassium silicate, which form glass when applied to wood, have been used to retard fire.^{7,8} Research suggests that these silicates can react with cell walls and limit leaching.⁹ When ignited, these silicates create a protective glass layer, improving wood's thermal stability and fire resistance.¹⁰

Silica gel, an example of a silicate fire retardant, offers benefits such as good water retention, cooling ability, non-toxicity, thermal and chemical stability and low cost.^{11–13} Silica gel can be used in inorganic and organic forms, with each having its advantages and drawbacks. Inorganic silica gel is inexpensive but has poor water absorption, while organic polymer gels offer excellent moisture retention and durability against heat but are expensive.¹⁴ In the field of fire protection, gel-based fire-retardant materials are commonly used in coal mines but are not often utilized for wood fire protection.^{15–18} Xue *et al.* have explored the use of gel-stabilized foam, created using water glass and sodium bicarbonate, to extinguish coal mine fires.¹⁹ However, the water retention of this foam has not been extensively studied. Fan *et al.*¹³ have modified water glass gels with polymers to produce plastic gels with improved water absorption and thermal resistance. The outcomes demonstrated that the plastogel, with improved water retention, cools the coal body and prevents its oxidative breakdown. Additionally, silica foam has been developed to adhere to the surface of solid combustible objects, providing a strong fire-retardant effect, although its rapid self-hardening time limits its practical application.^{20,21} To enhance wood's resistance to leaching and fire, Zhu *et al.* added nanosilica sol to fire retardants containing phosphorus.²² Despite these advancements, the flame-retardant mechanisms of these materials, including cooling, shielding and insulating, require further investigation.

In this study, considering the chemical stability of polyacrylamide (HPAM), its non-reactivity with the substances separated during the gelation process and its stability against pH and temperature variations, HPAM was chosen to be added to silica gel prepared with aluminum citrate and water glass solution to investigate its impact on water retention. Sodium polyacrylate molecules can

interweave into the silicate hydrogel through intermolecular interactions, forming an inorganic–organic interpenetrating network gel system. Various analytical approaches were used to examine the flame-retardant mechanism of silica gel, including analysis of elemental composition, functional groups and silica gel treated with wood components. The combustion morphology and mass loss of silica gel-treated wood were also examined to understand its macroscopic mechanism.

EXPERIMENTAL

Preparation of materials

Anionic polyacrylamide (HPAM, Shanghai Bidet Medical Technology Co., Ltd., China), gluconate-delta-lactone (GDL, Sahn Chemical Technology Shanghai Co., Ltd., China), aluminum citrate (AlCit, Beijing Enokai Technology Co., Ltd., China), inorganic salt sodium silicate solution (Sahn Chemical Technology Shanghai Co., Ltd., China), sodium bicarbonate (McLean Reagent Chemistry Co., Ltd., Shanghai, China) and deionized water mixed reaction made up the majority of the silica gel used in this study.

In Table I, one can see the ratios of different ingredients required to make silica gel for the tests.

TABLE I. Quantities of HPAM and GDL for the synthesis of silica gels ($m(\text{AlCit}) = 1.0 \text{ g}$, $m(\text{Na}_2\text{SiO}_3) = 8.0 \text{ g}$, $m(\text{NaHCO}_3) = 4.0 \text{ g}$ and $m(\text{deionized water}) = 87 \text{ g}$)

No.	GDL, g	HPAM, g
1	0.1	0.2
2	0.1	0.4
3	0.1	0.6
4	0.1	0.8
5	0.2	0.2
6	0.2	0.4
7	0.2	0.6
8	0.2	0.8
9	0.3	0.2
10	0.3	0.4
11	0.3	0.6
12	0.3	0.8

The process of preparing silica gel is outlined as follows: HPAM solutions were mixed with GDL (0.1, 0.2 and 0.3 wt. %) and AlCit (1.0 wt. %) at different concentrations (0.2, 0.4, 0.6 and 0.8 wt. %). Sodium silicate and sodium bicarbonate concentrations of 8 and 4 wt. %, respectively, were chosen based on previous studies on silica gel gelation.²³ The solution was stirred using a magnetic stirrer to ensure homogeneity. Sodium silicate was then added to the mixture to initiate the gelation process. The synthesized silica gel was vacuum-dried at 100 °C to remove excess water.

Characterizations and calculation

The water retention capacity of the silica gel was determined by placing the gel in a 100 °C oven and weighing it hourly over a 12-h period. This process was repeated for each sample

set, with the changes in mass being monitored hourly. The average water retention capacity was then calculated based on these measurements.

The following formula can be used to determine the water retention capacity of silica gel:²⁴

$$W = 100 \frac{M_1 - M_2}{M_1} \quad (1)$$

where W is the water retention percentage of silica gel, M_1 is the initial weight of silica gel and M_2 is the gel weight after every hour of drying.

XPS was used to analyze surface elements and their chemical states. The experiment used a homogeneous AlK α X-ray source at 1486.6 eV, with working pressure and analysis chamber vacuum levels set at 10^{-9} mbar and 5×10^{-7} Pa, respectively.

XRD diffractometer analyzed phase proportion, with a range of 5 to 90° (2θ), step size of 0.02° and settings of 40 kV, 40 mA and 5 °/min scanning speed.

Wood@gel samples were prepared by mixing silica gel with 100–200 mesh wood.¹⁹ Firstly, selected pine wood measuring 1 cm×1 cm×10 cm was dried in a vacuum drying oven at 70 °C for 12 h. The dried wood was then submerged in silica gel for ten minutes to enhance its fire resistance. For fire resistance testing, the samples were burned for one minute under the flame of an alcohol lamp. The percentage of weight loss was calculated to assess the fire resistance.

Tensor 37 infrared spectrometer was used to analyze functional group differences, with a scan range of 400 to 4000 cm^{-1} and an estimated accuracy of 4 cm^{-1} .

The Mettler simultaneous thermal analyzer measured dimensions during degradation. TGA applied 20 ml/min of air, heating from 30 to 800 °C at 10.0 °C/min using a 10.0±0.5 mg sample in a 70 μL alumina crucible.

The total weight loss percentage (W) is calculated according to Eq. (1), with M_1 and M_2 representing the sample's mass before and after the combustion test, respectively.

RESULTS AND DISCUSSION

Principles of silica gel generation

Silicic acid was created by the progressive combining of H^+ with the ions that were negative in the sodium silicate solution and by adding NaHCO_3 . The silicic acids polymerize with each other, as shown in Fig. 1a, to form polysilicic acid, which then transforms into silica gel with a spatially organized structure consisting of Si–O–Si linkages. During silica gel formation, intermolecular interactions between HPAM molecules and Si–O bonds can lead to the formation of a gel system with an organic–inorganic interpenetrating mesh structure (Fig. 1b). This increases the tensile strength of the silica gel. Additionally, the –COO– group of HPAM can coordinate with the polynucleated hydroxyl-bridged composite ions created by aluminum (Fig. 1b), which helps to form a strong network structure in the system and enhances the ability of silica gel to retain water.¹⁷

Water retention rate

Figs. 2a–c indicate that silica gels, prepared with a 0.4 wt% concentration of HPAM, demonstrated the highest water retention capacity when varying concen-

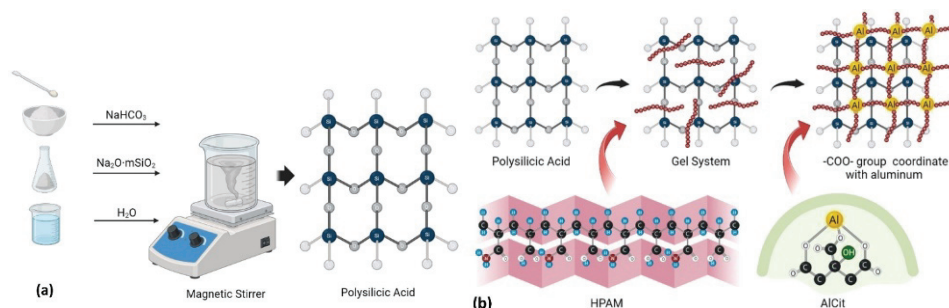


Fig. 1. The principle of silica gel generation: a) formation and structure of polysilicic acid; b) structural formation process of multinuclear hydroxyl-bridged composite ionic coordination networks.

trations of GDL (0.1, 0.2 and 0.3 wt. %) were utilized. Furthermore, at HPAM and GDL concentrations of 0.4 and 0.2 wt. %, respectively, the silica gel exhibited superior water retention as shown in Fig. 2d.

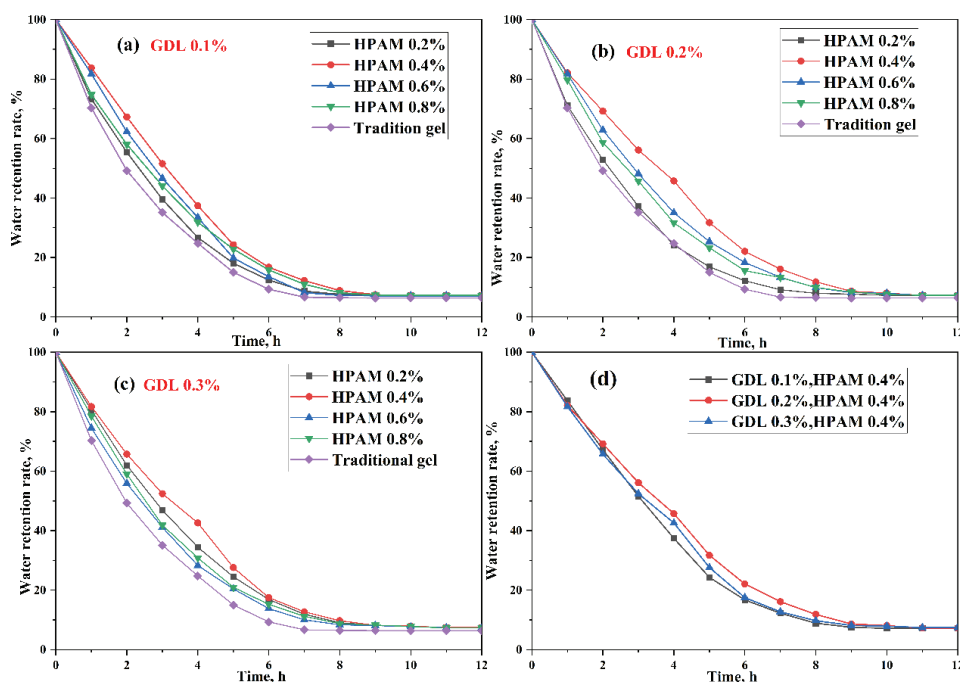


Fig. 2. Variation in silica gel water retention rates through heating time.

HPAM contributes to water retention through its ability to form a three-dimensional network that traps water molecules. At 0.4 wt. %, HPAM provides an optimal balance between viscosity and gel strength, ensuring sufficient network formation without overly increasing the viscosity, which could impede water

mobility within the gel. GDL acts as a gelling agent and pH adjuster. At 0.2 wt. %, GDL hydrolyzes to gluconic acid, gradually lowering the pH and facilitating the gelation process by promoting the cross-linking of HPAM chains. This concentration of GDL ensures a controlled and gradual gelation process, leading to a stable gel network.

The active hydrolysis and deprotonation of some $-\text{CONH}_2$ and $-\text{COOH}$ groups in HPAM result in increased electrostatic repulsion and elongation of the polymer chain. The hydrolysis of HPAM converts amide groups ($-\text{CONH}_2$) to carboxylic acid groups ($-\text{COOH}$), while deprotonation removes H^+ from carboxylic acid groups, forming carboxylate anions ($-\text{COO}^-$). $-\text{COO}^-$ forms strong hydrogen bonds with water, enhancing the stability of the polymer chain contacts. Therefore, the addition of the appropriate amount of HPAM contributes to the silica gel's excellent water retention properties.

XPS analysis

The sample with the best water retention (HPAM and GDL concentration of 0.4 and 0.2 wt. %) was analyzed using XPS. The results are displayed in Fig. 3a, revealing the composition of silica gel in terms of 1s and 2p electronic states. The 1s orbitals include O, Na and C, while Si and Al are present in the 2p orbitals. The Si 2p peak at 103.08 eV indicates that Si exists in the form of silica in the solution.

The C 1s spectrum of silica gel, illustrated in Fig. 3b, displays peaks corresponding to various groups. The spectrum shows an overlap of peaks for C–C and C–H, with the highest peak representing C–O, followed by C=O and O=C–O. Previous studies have indicated that hydrophilic functional groups such as C–O and C=O, as well as hydrophobic functional groups like C–C and C–H, are the primary functional groups in silica gel.²⁵ With 97 % or more of its functional groups being hydrophilic, the gel exhibits high hydrophilicity, enhancing its fire prevention effectiveness. The 97 % hydrophilic content was determined through XPS analysis of the C 1s spectrum. By integrating the peak areas for hydrophilic (C–O, C=O, O=C–O) and hydrophobic (C–C, C–H) groups, it was found that hydrophilic groups accounted for 97 % or more of the total peak area, indicating the gel's predominant hydrophilicity.

XRD analysis

Fig. 3c depicts the results of the X-ray diffraction analysis of the silica gel, with a broad peak at 22° indicating its typical amorphous state, consistent with the JCPDS phase identification card (PDF#27-0605).^{26,27}

Studies have shown that when silica gel is exposed to humid air, the hydroxyl groups of water molecules react with silica particles on its outermost layer, producing Si–OH groups.²⁸ The surface of SiO_2 has a high affinity for water

molecules due to the hydrophilic nature of hydroxyl groups. Additionally, the substantial surface area and small pores of silica facilitate the coverage of the entire outer layer by water molecules.²⁹ Consequently, the water present in silica gel is a combination of chemically and physically adsorbed water.

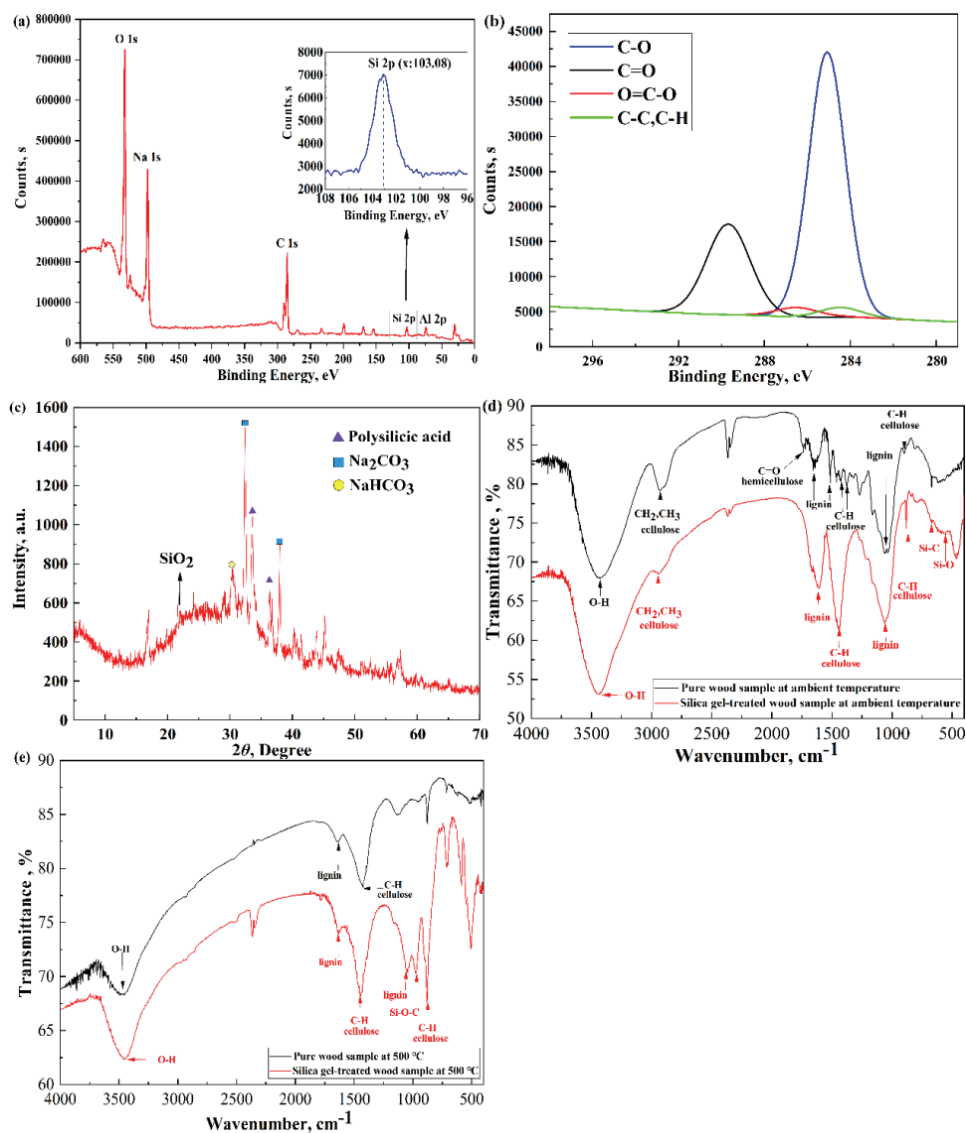


Fig. 3. Characterization of the microstructure of the samples: a) XPS wide energy scan spectrum of silica gel; b) C 1s XPS curve of silica gel; c) XRD graph of silica gel; d) FTIR testing of pure wood sample and silica gel-treated wood sample at ambient temperature; e) FTIR testing of pure wood sample and silica gel-treated wood sample at 500 °C.

Furthermore, Fig. 3c reveals the presence of polysilicic acid (PDF#27-0606) and Na_2CO_3 (PDF#08-0448) in the produced silica gel. The presence of Na_2CO_3 indicates the polymerization and reaction mechanism of silica gel discussed earlier in the preparative synthesis section. In this process, H^+ in the NaHCO_3 (PDF#15-0700) solution is absorbed by sodium silicate to produce polysilicate and sodium carbonate. Polysilicate helps the wood surface form a heat-stabilizing layer at high temperatures, thereby enhancing the wood's fire resistance. Therefore, silica gel is considered an effective fire retardant due to its ability to form such a protective layer:



FTIR analysis

Hemicellulose, cellulose and lignin are the primary components of wood.³⁰ There are four sets of experimental samples: unignited natural wood, unignited natural wood treated with silica gel, wood ignited by a 500 °C heat source and wood treated with silica gel and then ignited by a 500 °C heat source. Fig. 3d shows the FTIR spectrum of unignited natural wood and unignited natural wood treated with silica gel. In the spectrum of unignited natural wood, the peaks at 2930 cm^{-1} correspond to CH_2 and CH_3 groups. The C–H groups are distributed in three peaks at 1427, 1378 and 898 cm^{-1} , which are the main absorption peaks associated with cellulose. The peak at 1738 cm^{-1} indicates the C=O stretching vibration, characteristic of hemicellulose. The three major absorption peaks of lignin are observed at 1634, 1510 and 1053 cm^{-1} , representing the vibrations of the C–O stretching bond.

In comparison, the FTIR spectrum of the silica gel-treated wood shows additional peaks at 553 and 669 cm^{-1} . The peak at 553 cm^{-1} indicates the presence of silica gel in the wood, while the peak at 669 cm^{-1} corresponds to the Si–C stretching vibration, suggesting a chemical connection between silica gel and wood components. These additional peaks are not present in the untreated wood spectrum. The presence of Si–O and Si–C bonds in the treated wood leads to the formation of thick, highly heated charred layers, acting as a barrier that retards the burning process by limiting the dispersion of flammable volatile components and heat transfer.³¹

Fig. 3e displays the FTIR results of wood samples ignited by a 500 °C heat source, including the both untreated and silica gel-treated samples. In the spectrum of untreated wood ignited at 500 °C, only the 1427 cm^{-1} cellulose absorption peak remains, while the peaks of hemicellulose and lignin vanish or are reduced. This indicates that lignin pyrolysis is essentially complete at 500 °C, with the system continuing to pyrolyze and deoxygenate, forming charcoal progressively.

In comparison, the FTIR spectrum of the silica gel-treated wood heated at 500 °C shows that the cellulose retains an absorption peak at 898 cm^{-1} , demon-

strating improved thermal resilience. The lignin peak at 1510 cm^{-1} is only partially lost and new peaks at 715 and 976 cm^{-1} , characteristic of the Si–C and the Si–O–C bonds, respectively. In addition to the Si–O and the Si–C bonds described above, the thermal stability of Si–O–C has been also demonstrated in the literature.³² Hence, the presence of these bonds indicates the formation of charred layers at high temperatures, effectively halting the decomposition and burning of wood. Therefore, silica gel exhibits excellent fire-retardant properties, as the treated wood still contains cellulose and lignin that are not completely broken down $500\text{ }^{\circ}\text{C}$.

TGA-DTG analysis

To evaluate the thermal resistance, charring prospects and decomposition rate of wood, TGA analysis can be employed. TGA analysis was conducted to investigate the thermal stability, charring ability and degradation rate of wood, silica gel and wood@gel in an air atmosphere (Fig. 4). The thermogravimetric (TG) and differential thermogravimetric (DTG) analyses in Fig. 4 reveal three phases in the thermal degradation of wood. The initial stage ($30\text{--}130\text{ }^{\circ}\text{C}$) involves the evaporation of water molecules, causing a 6 % mass loss. In the second charring stage ($160\text{--}360\text{ }^{\circ}\text{C}$, peak at $317\text{ }^{\circ}\text{C}$), the weight decreases significantly from 94 to 33 % as hemicellulose and cellulose decompose into char residues, releasing CO_2 , CO , CH_4 , CH_3OH and $\text{C}_2\text{H}_5\text{OH}$.² The third stage ($360\text{--}500\text{ }^{\circ}\text{C}$, peak at $437\text{ }^{\circ}\text{C}$) involves calcination, with a residual percentage of 4.9 % due to the decomposition of lignin and oxidation of char residue from the second stage.³³

The wood@gel sample exhibits a 5 % mass loss in the first stage ($30\text{--}130\text{ }^{\circ}\text{C}$) due to water evaporation. In the second stage ($130\text{--}500\text{ }^{\circ}\text{C}$), wood@gel shows a high residual carbon rate of 56 %, attributed to the oxidized breakdown of cellulose and hemicellulose. Compared to pure wood, wood@gel loses weight more slowly in this phase, indicating the protective effect of silica gel. The maximal breakdown temperature of wood@gel in the second stage is $263\text{ }^{\circ}\text{C}$, according to the DTG curve (Fig. 4b) and the third stage breakdown can reach $580\text{ }^{\circ}\text{C}$, suggesting silica gel's involvement in wood decomposition. In contrast, the dehydration of surface Si–OH groups on silica gel is principally responsible for the third stage mass loss of wood@gel, which results in a residual carbon rate that is 41 % greater than that of pure wood. The preservation of cellulose and delay of pyrolysis reaction in wood are attributed to the charred layer produced by silica gel during combustion, as noted by Rowell, Miyafuji and Saka, which obstructs blazing and smoldering combustion by limiting oxygen and combustible product access.^{34,35}

The flame-retardant mechanism of wood@gel involves the formation of multi-coordination organosilicon compounds with polyhydroxy cellulose at high temperatures, hindering thermal movement between cellulose macromolecular

chains, reducing the pyrolysis rate and enhancing thermal stability.³⁶ Additionally, the creation of a protective carbonized layer with Si–O, Si–O–C and Si–C linkages between the silicon-containing compound and wood improves thermal stability.

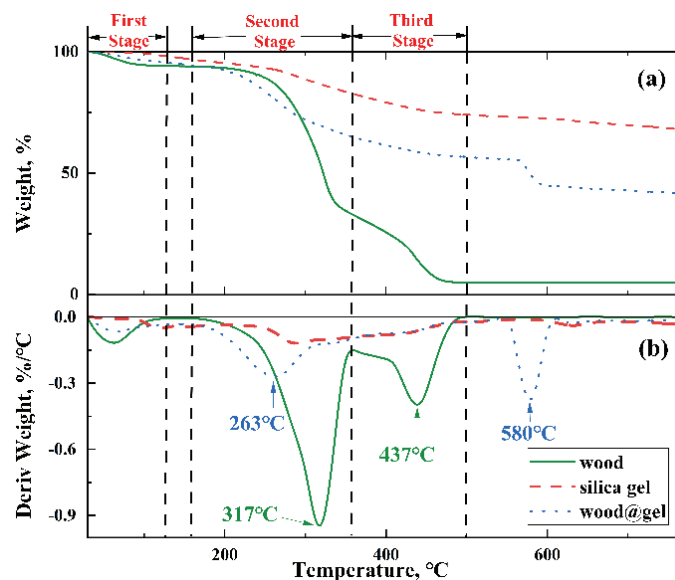


Fig. 4. Wood, silica gel and wood@gel samples' TG (a) and DTG (b).

Fire resistance analysis

Using natural wood (sample 1#) and wood treated with silica gel (sample 2#), we investigated silica gel's ability to delay flames on wood. Both samples were exposed to the flame of an alcohol lamp as described in the fire resistance analysis section. The results depicted in Fig. 5 indicate that sample 1# ignited after 6 seconds and even though the alcohol lamp was removed after 60 s, it took 197 s for the flame to extinguish. This prolonged burning was mainly due to the complete decomposition of the active ingredients present in wood, such as cellulose, hemicellulose and other wood elements. Conversely, under the same flame conditions, sample 2# did not exhibit any combustion phenomena for 60 s after ignition, as shown in Fig. 5. The presence of silica gel on the wood's surface led to the development of a protective charred coating that effectively prevented further burning.

Table II presents the mass loss of samples before and after combustion. Samples 1# and 2# experienced total mass losses of 76 and 23 %, respectively. The addition of silica gel reduced the mass loss rate by 70 % in sample 2#, attributed to the formation of a protective layer via Si–O, Si–O–C and Si–C linkages on its external layer during burning. This coating enhances the wood's fire resistance.

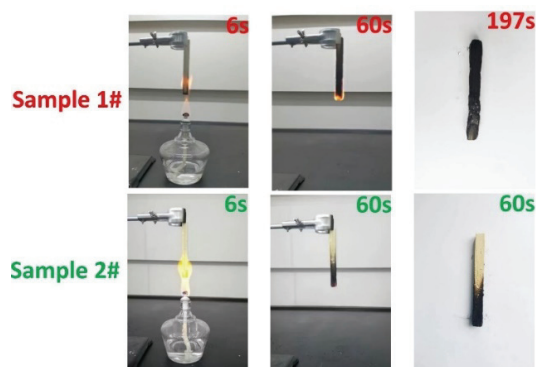


Fig. 5. Experiment testing the resistance to fire.

TABLE II. Burning mass reduction velocity at the fire resistance test

Sample	1#			2#		
Pre-burning, g	4.72	4.84	4.80	4.95	4.97	4.99
Post-burning, g	1.10	1.24	1.09	3.90	3.73	3.84
Mass loss rate, %	76.69	74.38	77.29	21.21	24.95	23.05
Average mass loss rate, %	76.12			23.07		

CONCLUSION

In this investigation, various ratios of HPAM and GDL were utilized to assess the water retention and flame-retardant properties of silica gel on wood. Maximum water retention was observed at 0.4 wt. % HPAM and 0.2 wt. % GDL. To better understand these properties, we conducted combustion experiments and microscopic mechanism studies.

The combustion experiments show that silica gel forms a barrier that isolates oxygen and heat from reaching the wood surface. Additionally, silicon increases the thermal stability of the carbon layer during the wood carbonization process, acting as a flame retardant. Microscopic mechanism studies show that hydrophilic groups C–O and C=O on the surface of silica gel contribute to its excellent hydrophilicity. After the wood combustion, the formation of Si–O, Si–O–C and Si–C bonds on the surface increases the thermal stability of the carbon layer, revealing the flame-retardant mechanism of the carbon layer. The results demonstrated silica gel reduces mass loss in treated wood at high temperatures by 36 % (TG analysis) and 53 % (fire resistance testing) respectively, showing its efficacy as a fire retardant.

Acknowledgment. This work was supported by the Postgraduate Research & Practice Innovation Program of Jiangsu Province (grant number KYCX23_1498).

ИЗВОД

ПОВЕЋАЊЕ ОТПОРНОСТИ ДРВЕТА НА САГОРЕВАЊЕ ПОМОЋУ СИЛИКА ГЕЛА СА ВЕЛИКИМ ЗАДРЖАВАЊЕМ ВОДЕ: ОБЕЋАВАЈУЋЕ РЕШЕЊЕ ЗА УСПОРАВАЊЕ САГОРЕВАЊА

ZHONGBIN FEI, YINGNAN ZHANG, ZHI WANG, YILING DUAN и BIN ZHANG

International Center for Chemical Process Safety, Nanjing Tech University, Nanjing, 211816, China

У овом раду је испитивано задржавање воде и могућност успоравања сагоревања силика гела припремљеног коришћењем анјонског полиакриламида (НРАМ), глуконат-делта-лактона (GDL) и алуминијум-цитрата (AlCit). Узорци силика гела су синтетисани коришћењем натријум-силиката (8 мас. %), натријум-хидрогенкарбоната (4 мас. %) и различитих количина НРАМ (0,2–0,8 мас. %) и GDL (0,1–0,3 мас. %). Гелови су окарактерисани следећим техникама: XPS, XRD, FTIR и TGA. Оптимално задржавање воде је постигнуто при 0,4 мас. % НРАМ и 0,2 мас. % GDL. Овај гел садржи, у поређењу са традиционалним геловима, више површинске воде захваљујући већем броју хидрофилних група и аморфној природи. На високим температурама силика гел формира слој са угљеником који настаје сагоревањем дрвета, спречавајући продирање кисеоника, што минимизира даље сагоревање. Након сагоревања на 500 °C, губитак масе дрвета третираног силика гелом је 36–53 % мањи у поређењу са нетретираним дрветом, што указује на ефикасност силика гела у спречавању даљег сагоревања.

(Примљено 14. априла, ревидирано 10. јуна, прихваћено 23. августа 2024)

REFERENCES

1. T. Farid, M. I. Rafiq, A. Ali, W. Tang, *EcoMat* **4** (2022) e12154 (<https://doi.org/10.1002/eom2.12154>)
2. S. He, W. Wu, M. Zhang, H. Qu, J. Xu, *J. Therm. Anal. Calorim.* **128** (2017) 825 (<https://doi.org/10.1007/s10973-016-5947-z>)
3. E. Baysal, M. K. Yalinkilic, M. Altinok, A. Sonmez, H. Peker, M. Colak, *Constr. Build. Mater.* **21** (2007) 1879 (<https://doi.org/10.1016/j.conbuildmat.2006.05.026>)
4. I. Ratajczak, B. Mazela, *Holz Als Roh Werkst.* **65** (2007) 231 (<https://doi.org/10.1007/s00107-006-0154-4>)
5. Q. Fu, D. S. Argyropoulos, D. C. Tilotta, L. A. Lucia, *J. Anal. Appl. Pyrolysis* **81** (2008) 60 (<https://doi.org/10.1016/j.jaap.2007.08.003>)
6. H. Yamaguchi, *Wood Sci. Technol.* **36** (2002) 399 (<https://doi.org/10.1007/s00226-002-0149-1>)
7. A. M. Pereyra, C. A. Giudice, *Fire Saf. J.* **44** (2009) 497 (<https://doi.org/10.1016/j.firesaf.2008.10.004>)
8. G. Canosa, P. V. Alfieri, C. A. Giudice, *J. Fire Sci.* **29** (2011) 431 (<https://doi.org/10.1177/0734904111404652>)
9. S. Nami Kartal, W. J. Hwang, A. Yamamoto, M. Tanaka, K. Matsumura, Y. Imamura, *Int. Biodeterior. Biodegrad.* **60** (2007) 189 (<https://doi.org/10.1016/j.ibiod.2007.03.002>)
10. S. Hribernik, M. S. Smole, K. S. Kleinschek, M. Bele, J. Jamnik, M. Gaberscek, *Polym. Degrad. Stabil.* **92** (2007) 1957 (<https://doi.org/10.1016/j.polymdegradstab.2007.08.010>)
11. S. G. Hu, S. Xue, *J. Coal Sci. Eng. China* **17** (2011) 256 (<https://doi.org/10.1007/s12404-011-0306-y>)
12. M. Wu, Y. Liang, Y. Zhao, W. Wang, X. Hu, F. Tian, Z. He, Y. Li, T. Liu, *Colloids Surfaces, A* **629** (2021) 127443 (<https://doi.org/10.1016/j.colsurfa.2021.127443>)

13. Y. Fan, Y. Zhao, X. Hu, M. Wu, D. Xue, *Fuel* **263** (2020) 116693 (<https://doi.org/10.1016/j.fuel.2019.116693>)
14. S. Hu, S. Xue, *J. Coal. Sci. Eng. China* **17** (2011) 256 (<https://doi.org/10.1007/s12404-011-0306-y>)
15. B. Qin, G. Dou, Y. W. H. Wang, L. Ma, D. Wang, *Fuel* **190** (2017) 129-135 (<https://doi.org/10.1016/j.fuel.2016.11.045>)
16. P. Qian, Z. Qin, H. Guo, C. Geng, N. Yan, X. Cui, *Ind. Saf. Environ. Prot.* **38** (2012) 13 (https://caod.oriprobe.com/articles/30918095/Sodium_Silicate_polyelectrolyte_Composite_Gel_Mate.htm)
17. X. Ren, X. Hu, D. Xue, Y. Li, Z. Shao, H. Dong, W. Cheng, Y. Zhao, L. Xin, W. Lu, *J. Hazard. Mater.* **371** (2019) 643 (<https://doi.org/10.1016/j.jhazmat.2019.03.041>)
18. K. Wang, W. Lu, Y. Du, Q. Zhang, J. Xu, *Min. Saf. Environ. Prot.* **43** (2016) 8 (<http://www.cnki.net/kcms/detail/50.1062.TD.20160202.1908.006.html>)
19. D. Xue, X. Hu, W. Cheng, J. Wei, Y. Zhao, L. Shen, *Fuel* **264** (2020) 116903 (<https://doi.org/10.1016/j.fuel.2019.116903>)
20. D. S. Kuprin, *J. Sol-Gel Sci. Technol.* **81** (2017) 36 (<https://doi.org/10.1007/s10971-016-4285-8>)
21. A. V. Vinogradov, D. S. Kuprin, I. M. Abduragimov, G. N. Kuprin, E. Serebriyakov, V. V. Vinogradov, *ACS Appl. Mater. Interfaces* **8** (2016) 294 (<https://doi.org/10.1021/acsami.5b08653>)
22. X. Zhu, Y. Wu, C. Tian, Y. Qing, C. Yao, *J. Nanomater.* **2014** (2014) 1 (<https://doi.org/10.1155/2014/867106>)
23. Y. Zhang, M. Jing, M. Zhang, S. Hou, B. Zhang, *Fire Technol.* **58** (2022) 3597 (<https://doi.org/10.1007/s10694-022-01334-y>)
24. Y. Liu, M. Wang, S. Zhao, Y. Liu, J. Yang, *J. Shandong Univ. Sci. Technol. (Nat. Sci.)* **37** (2018) 26 (<https://kns.cnki.net/kcms/detail/37.1357.N.20180509.1327.012.html>)
25. W. Xia, J. Yang, C. Liang, *Appl. Surf. Sci.* **293** (2014) 293 (<https://doi.org/10.1016/j.apsusc.2013.12.151>)
26. M. A. Abou Rida, F. Harb, *J. Met. Mater. Miner.* **24** (2014) 37 (<https://www.jmmm.material.chula.ac.th/index.php/jmmm/article/view/108>)
27. S. He, Y. Huang, G. Chen, M. Feng, H. Dai, B. Yuan, X. Chen, *J. Hazard. Mater.* **362** (2019) 294 (<https://doi.org/10.1016/j.jhazmat.2018.08.087>)
28. R. L. DeRosa, P. A. Schader, J. E. Shelby, *J. Non-Cryst. Solids* **331** (2003) 32 (<https://doi.org/10.1016/j.jnoncrysol.2003.08.078>)
29. X. Chen, G. Zhu, J. Wang, Q. Chen, *Bull. Chin. Ceram. Soc.* **36** (2017) 4044 (<http://gsybt.jtxb.cn/EN/Y2017/V36/I12/4044>)
30. D. C. O. Marney, L. J. Russell, R. Mann, *Fire Mater.* **32** (2008) 357 (<https://doi.org/10.1002/fam.973>)
31. Y. Zhang, M. Jing, M. Zhang, S. Hou, Y. Gong, J. Jiang, B. Zhang, *Silicon* **14** (2022) 12633 (<https://doi.org/10.1007/s12633-022-01975-2>)
32. Y. Yang, CN 107805447 A (2017)
33. M. Uddin, K. Kiviranta, S. Suvanto, L. Alvila, J. Leskinen, R. Lappalainen, A. Haapala, *Fire Saf. J.* **112** (2020) 102943 (<https://doi.org/10.1016/j.firesaf.2019.102943>)
34. R. M. Rowell, *The chemistry of solid wood*, American Chemical Society, Washington, DC, 1984, pp. 531–574 (<https://doi.org/10.1021/ba-1984-0207>)
35. H. Miyafuji, S. Saka, *J. Wood Sci.* **47** (2001) 483 (<https://doi.org/10.1007/BF00767902>)
36. D. H. Blount, US 4380592 A (1983).